Elongational Rheology of Polyethylene Melts

B. SEYFZADEH,[1] J. R. COLLIER[2]

[1] Center for Advanced Engineering Fibers and Films, Clemson University, South Carolina 29634-0909

[2] Chemical Engineering Department, University of Tennessee at Knoxville, Knoxville, Tennessee 37996-2200

Received 25 April 2000; accepted 24 May 2000

ABSTRACT: Effective elongational viscosities were measured for high- and low-density polyethylene samples using a capillary rheometer fitted with semihyperbolic dies. These dies establish a purely elongational flow field at constant elongational strain rate. The effective elongational viscosities were evaluated under the influence of the process strain rate, Hencky strain, and temperature. Enthalpy and entropy changes associated with the orientation development of semihyperbolic-processed melts were also estimated. The results showed that elongational viscosities were primarily affected by differences in the weight-average molecular weight rather than in the degree of branching. This effect was process-strain-rate- as well as temperature-dependent. An investigation of the melt-pressure relaxation and the associated first decay time constants revealed that with increasing strain rate the molecular field of the melt asymptotically gained orientation in approaching a limit. As a result of this behavior, molecular uniqueness became much less distinct at high process strain rates, apparently yielding to orientation development and the associated restructuring of the melt's molecular morphology. © 2001 John Wiley & Sons, Inc. J Appl Polym Sci 79: 2170–2184, 2001

Key words: elongational viscosity; semihyperbolic die; capillary extrusion; pressure relaxation; flow-induced orientation

INTRODUCTION

Whereas the field of shear rheology has been well established and numerous publications are communicated through respected journals, the related and important branch of elongational rheology is still at an early development stage. However, some valuable results have been reported from various groups, especially for the extensional flow of polyolefins.[1–4] Other investigators[5,6] published results on the relation of elongational deformation to flow-induced crystallization of poly(ethylene terephthalate) (PET) and poly(ethylene naphthalate) (PEN). Relevant findings were also reported on the elongational properties of polymer melts by gravity spinning,[7] spinline measurements for elongational material characterization,[8] extensional rheometry of polymer multilayers,[9] elongational viscosities of random and block copolymer melts,[10] uniaxial elongational flow of particle-filled polymer melts,[11] polymer stretching in an elongational flow,[12] and uniaxial extensional characterization of a shear-thinning fluid using axisymmetric flow birefringence.[13]

Elongational melt-flow behavior is an important and fundamental concept underlying many industrial plastics operations that involve a rapid change of shape.[14] Examples include fiber spinning, extrusion through converging nozzles, film stretching and blowing, bottle blowing, and injection molding. Although in many of these processes the elongational flow dominates, shearing

Correspondence to: J. R. Collier.

Journal of Applied Polymer Science, Vol. 79, 2170–2184 (2001)

effects almost always accompany it. This implies that it is inherently difficult to establish, control, and measure a purely elongational flow field. This statement may also be reworded by saying that it is difficult to prevent, compensate, or measure shearing effects that occur along with the elongational flow. Moreover, most elongational rheometers operate at elongational rates at least an order of magnitude below those of industrial processes.

When polymer melts are subjected to processing operations such as those mentioned in the previous paragraph, the material experiences enormous stresses which force the macromolecular matrix to gain considerable orientation, that is, the molecular chains align in a more orderly close-packed fashion. This event has significant effects on the melt-flow behavior and can be measured in terms of effective elongational viscosity and changes in the entropy and enthalpy. The orientation development also determines the final product's mechanical and bulk properties such as the resistance to stresses, toughness, and degree of crystallinity. Knowledge of a polymeric material's elongational melt-flow behavior in the form of these measurable parameters is useful information in terms of selecting an adequate polymer grade for a particular application when expecting desired product properties. Moreover, the ability to quantitatively assess the forces that result in an orientation-developing flow profile opens the possibility for on-line process control with fast parameter adjustments and material property selection. Since there is a large number of polymer classes and grades commercially available to plastics processing clients, there are also many material properties to choose from. Rheology is sensitive to polymer attributes including molecular weight, molecular weight distribution, degree of side-chain branching, and achievable degree of crystallinity. How these characteristics are brought about depends much on the operating parameters and conditions during the polymerization and subsequent processes. It is expected that material properties will affect the elongational melt-flow behavior. Hence, such molecular characteristics should be related to the previously mentioned measurable elongational flow variables.

Previous research in this group[15] brought forth that polymer melts can be elongationally characterized at processing strain rates. The method involved coextrusion of a polypropylene core with a polyethylene (PE) skin, where the skin with its much lower viscosity functioned as a lubricating layer to dissipate shearing effects at the wall. Using a hyperbolic slit and a semihyperbolic conical die, measurements showed that the core was essentially in a purely elongational flow at a constant strain rate. Further attempts to find a correction factor for skinless extrusion led to the conclusion that the orientation-developing effects of the melt are so substantial that shearing gradients near the wall become comparatively insignificant.[14] As a continuation of these previously established results, the concept of purely elongational flow imposed by the unique semihyperbolic contour profile is now applied to a broader class of materials. PEs are at the center of interest for which elongational flow characteristics and molecular orientation are investigated in view of macromolecular characteristics.

THEORETICAL BASIS TO DATA ACQUISITION

The theoretical foundation for the analysis of elongational melt-flow data was established previously in this group by Collier et al.[14] for the semihyperbolic converging die geometry. To facilitate the reader with a better understanding of those concepts underlying the data processing and the results to be discussed, the theoretical development is sketched out here. A complete and detailed analysis is to be found in Collier et al.'s publication.

The semihyperbolic die was designed for the melt or solution to maintain a constant elongational strain rate throughout the core. This is accomplished by describing the channel surface with the equation $R^2z = C$, where z is the axial flow direction; R, the radius of the flow channel; and C, a constant. Two of the semihyperbolic dies used in this research were ones having a Hencky strain, ε_h, equal to 6 and 7. The Hencky strain is defined as the natural logarithm of the die entrance area to the exit area; therefore, $\varepsilon_h = 6$ corresponds to an area ratio of approximately 400 and $\varepsilon_h = 7$ to 1100.

When the melt flows through the semihyperbolic channel, it assumes the shape of the die surface, that is, layers of the melt may be viewed as stream lines experiencing the same conditions. These streamlines can be described by the stream function, Ψ, forming a two-dimensional surface. The stream function is defined to satisfy the continuity equation, and in shear free flow, the po-

tential function, Φ, satisfies the irrotationality equation, and for pressure-driven flow, it describes a constant pressure surface. Both functions, Ψ and Φ, are mutually orthogonal. For the axisymmetric die geometry and cylindrical coordinate system, stream and potential functions are defined respectively as

$$\Psi = -\frac{\dot{\varepsilon}}{2} r^2 z \tag{1}$$

$$\Phi = \dot{\varepsilon}\left(\frac{r^2}{4} - \frac{z^2}{2}\right) \tag{2}$$

The melt pressure, P, is directly proportional to $\rho\dot{\varepsilon}\Phi$, where $\dot{\varepsilon}$ is the elongational strain rate and ρ is the density. The velocity components in cylindrical coordinates were given in Bird et al.[16] as

$$v_z = -\frac{1}{r}\frac{\partial\Psi}{\partial r} = -\frac{\partial\Phi}{\partial z} = \dot{\varepsilon} z \tag{3}$$

$$v_r = \frac{1}{r}\frac{\partial\Psi}{\partial z} = -\frac{\partial\Phi}{\partial r} = -\frac{\dot{\varepsilon}}{2} r \tag{4}$$

with the nonzero velocity components being

$$\frac{\partial v_z}{\partial z} = \dot{\varepsilon}, \quad \frac{1}{r}\frac{\partial(r v_r)}{\partial r} = -\dot{\varepsilon}, \quad \frac{\partial v_r}{\partial r} = -\frac{\dot{\varepsilon}}{2} \tag{5}$$

The fundamental equations describing the flow are the conservation laws of mass, momentum, and energy and the irrotationality equation for potential flow. Moreover, an internal body force term must be taken into account. It represents the force per unit volume related to the orientation development and can be viewed as the force necessary to overcome the resistance toward developing the orientation imposed onto the melt by the converging shape of the die. As mentioned earlier, the semihyperbolic shape is one that provides a constant strain rate and constant resulting stress. The flow is therefore homogeneous and at constant acceleration as shown by the velocity gradient equations. This is not the case in shearing flow where a stress gradient acts in normal direction to the sheared surface and the stress tensor includes a shearing component gradient. Because of the constant elongational strain rate and strong dominance of the orientation development, the flow through the semihyperbolically converging die is expected to be essentially purely elongational. The only significant nonzero velocity gradients are in flow and transverse directions; hence, the only significant nonzero components of the deformation rate tensor, Δ, are the normal components.

Apart from what has been mentioned above, the theoretical development is founded on the following considerations:

1. The strain-rate state determines the stress state, that is, the flow behavior is dominant. Moreover, the die geometry, assuming negligible shearing gradients, dictates that the only significant nonzero deformation rate components are the normal components and these components are not a function of position, that is, the flow is homogeneous. Therefore, since the flow is homogeneous, the only significant nonzero stress components are the normal components and the stress components are not a function of the position. Thus, $\nabla \cdot \underset{\sim}{\tau} = 0$.
2. The melt is incompressible; therefore, $\nabla \cdot \underset{\sim}{v} = 0$.
3. The system is in an isothermal state; therefore, $\nabla \cdot \underset{\sim}{q} = 0$.
4. The flow is steady state; therefore, $\partial/(\partial t) = 0$.
5. The inertial terms are negligible; therefore, $\underset{\sim}{v}\nabla\underset{\sim}{v} = 0$ *and* $\nabla(v^2/2) = 0$.

The constant elongational strain rate of the flow channel forces the axial and transverse normal components of the stress tensor, τ_{zz} and τ_{rr}, to be constant. Their values depend on the strain rate. Experimental data for these semihyperbolically converging dies has proven that the body-force term strongly dominates shearing effects and thus causes the shear stress gradient to be negligible. This dominance along with the constant strain rate implies that the stress gradients in the momentum balance are negligible. Furthermore, this coupled with the low Reynolds number implies that the inertial terms are also negligible. With the previous statement of pressure P being proportional to $\rho\dot{\varepsilon}\Phi$, the momentum balance reduces to the statement that the pressure gradient is equal to the body-force term:

$$\frac{\partial P}{\partial r} = b_r \quad \text{and} \quad \frac{\partial P}{\partial z} = b_z \tag{6}$$

Furthermore, since

$$v_z = \dot{\varepsilon} z \quad \text{and} \quad \varepsilon_h = \ln\left(\frac{r_0^2}{r_e^2}\right) \tag{7}$$

the energy balance can be integrated from entrance to exit, and the stress component in cylindrical coordinates gives

$$\tau_{zz} = \frac{2}{3}\frac{\Delta P}{\varepsilon_h} + \frac{2}{3}\frac{\rho \Delta \hat{H}}{\varepsilon_h} = \frac{2}{3}\frac{\Delta P}{\varepsilon_h} + \frac{2}{3}\frac{\Delta H}{\varepsilon_h} \tag{8}$$

The pressure drop, ΔP, is defined as the entrance minus exit pressure, and ΔH is defined as the exit minus entrance enthalpy change per unit volume. The elongational viscosity, η_e, is defined in cylindrical coordinates as

$$\eta_e = \frac{\tau_{zz} - \tau_{rr}}{\dot{\varepsilon}} = \frac{3}{2}\frac{\tau_{zz}}{\dot{\varepsilon}} \tag{9}$$

Combining eqs. (8) and (9) gives

$$\eta_e = \frac{\Delta P}{\dot{\varepsilon}\varepsilon_h} + \frac{\rho \Delta \hat{H}}{\dot{\varepsilon}\varepsilon_h} = \frac{\Delta P}{\dot{\varepsilon}\varepsilon_h} + \frac{\Delta H}{\dot{\varepsilon}\varepsilon_h} \tag{10}$$

The enthalpy term represents either a real phase change or an apparent one that may be induced by the orientation-developing process in the melt. The effective elongational viscosity, η_{ef}, is related to η_e by

$$\eta_{ef} = \frac{\Delta P}{\dot{\varepsilon}\varepsilon_h} \tag{11}$$

$$\eta_e = \eta_{ef} + \frac{\Delta H}{\dot{\varepsilon}\varepsilon_h} \tag{12}$$

Therefore, the definition for the effective elongational viscosity includes any potential enthalpy change. The elongational strain rate is defined as

$$\dot{\varepsilon} = \frac{v_0}{L}(\exp \varepsilon_h - 1) \tag{13}$$

In eq. (13), ε_h is the Hencky strain as previously defined; L, the centerline length of the die; and v_0, the initial velocity.

The enthalpy change associated with the orientation development in the melt can be calculated as follows: Making the assumption that the non-Newtonian character of the melt in excess of that caused by the shear viscosity, η_s, at an equal value of shear rate is due to the resistance toward orientation, the actual Trouton ratio would be $\eta_e/\eta_s = 3$. Hence, the elongational viscosity can be expressed in terms of a measured shear viscosity and combined with eq. (12) to give

$$\Delta H = -\varepsilon_h \dot{\varepsilon}(\eta_{ef} - 3\eta_s) \tag{14}$$

The entropy change, ΔS, is an indicator as to what extent orientation develops. It can be determined using $\Delta G = \Delta H - T\Delta S$, where ΔG is the Gibbs free energy and T is the absolute temperature. Assuming that due to orientation development the flow reaches a quasi- or transient steady-state equilibrium, then $\Delta G = 0$ and

$$\Delta S = \frac{\Delta H}{T} \tag{15}$$

MATERIALS, EQUIPMENT, AND METHODOLOGY

The melt-flow behavior of selected PEs having unique molecular characteristics was investigated with the aid of an Advanced Capillary Extrusion Rheometer (ACER) made by Rheometric Scientific®, Inc. The instrument provides data for shear viscosities at varying strain rates when using straight capillary dies, and when fitted with the semihyperbolic dies, it enables the determination of effective elongational viscosities based on recorded equilibrium melt pressures. The ACER deforms a sample by forcing it through a capillary channel, and from the measurement, an apparent viscosity can be calculated. The flow of the melt is accomplished by a ram that moves at constant velocity through a precisely bored, preheated, cylindrical barrel of a known diameter. A pressure transducer located just above the entrance of the die measures the melt pressure and communicates the measured signals to the computer. A measurement at a set strain rate comes to completion when the pressure has reached an equilibrium plateau.

In addition to the elongational characterization, shear data needed to be obtained to calculate the enthalpy and entropy changes of the orientation-gaining molecular matrix as proposed in eqs. (14) and (15). This task was accomplished at a shear rate comparable in magnitude to the elongational rate using a Bohlin VOR shear rheome-

Table I Polymer Grades and Their Molecular Characteristics

Material Samples	MI (g/10 min)	Density (g/cm^3)	MW GPC Analyzed	MWD GPC Analyzed
LDPE-A	1.2	0.9	97,550	2.22
LDPE-B	7.5	0.9	56,950	1.99
LDPE-C	2.2	0.895	83,350	2.24
LDPE-D	2.3	0.919	86,650	6.85
LDPE-E	2.0	0.923	80,350	5.15
HDPE-A	0.3	0.943	105,200	9.74
HDPE-B	0.3	0.95	125,400	8.09
HDPE-C	0.3	0.954	125,700	13.00
HDPE-D	0.1	0.949	183,200	14.77
HDPE-E	0.1	0.949	154,100	12.63

ter in the steady and dynamic measuring modes with parallel-plate geometry.

The acquisition of polymeric materials required a careful selection of class-representative, uniquely defined polymer grades to meet the research objective. Knowledge of the molecular differences among the chosen high-density PEs (HDPEs) and low-density PEs (LDPEs) was essential to characterize the polyolefin class-representative melt-flow behavior and to interpret the results relevant to the research objective. All samples were commercially manufactured. The known molecular specifications are summarized in Table I. The manufacturers did not provide any information on branching characteristics. To establish meaningful comparisons between the effects of molecular weight versus branching on the elongational melt-flow behavior, at least a relative order of the extent of branching needed to be determined. This was accomplished by comparing the crystalline peak melt temperatures and relating these to the known polymer densities. Polymers are expected to display peak melt temperatures in accordance with their ability to crystallize. This will depend on the degree of branching because highly branched polymers (low-density) are sterically too hindered and insufficiently able to fold and pack tightly to crystallize to as high a level as are low-branched (high-density) polymers. A highly crystallized, well-ordered sample will require a higher melt temperature to become disordered through melting than does a low-crystallinity sample. Thus, the degree of branching is expected to decrease with an increase in the peak melt temperature. Whereas the quality or perfection of crystallinity relates to the crystalline peak melt temperature as just described, the extent or degree of crystallinity will depend on the measured thermal energy requirement, that is, the enthalpy change, necessary to accomplish melting. This enthalpy change is related to the area under the melt peak. When investigating HDPE and LDPE under the said criteria using differential scanning calorimetry (DSC), the results allowed us to establish a branching order which for the HDPE samples was A > D > E > B > C and for the LDPE samples was C > A > B > D > E. This order is consistent with the densities of these samples, the more branched samples in each sequence having a lower density than that of the less branched.

DISCUSSION

HDPE and LDPE samples were elongationally characterized using the Hencky 6 semihyperbolic die geometry at temperatures of 175, 200, 225, and 250°C. These temperatures were chosen because they cover a typical PE processing temperature range. Elongational strain rates were chosen as to cover as wide of a strain sweep as possible. For each polymer grade, the same 10 rates were applied. If a particular grade could not be extruded at high strain rates, the upper limit on the strain rate was dictated by the transducer's upper safety threshold pressure limitation of 35 MPa. The equilibrium pressures were recorded and the elongational viscosities were determined as described previously.

Graphs of effective elongational viscosity dependence on the elongational strain rate were prepared and are shown in Figures 1–4 for the HDPE samples and in Figures 5–8 for the LDPE samples. In all cases, the viscosities decreased in a non-Newtonian power-law fashion with increas-

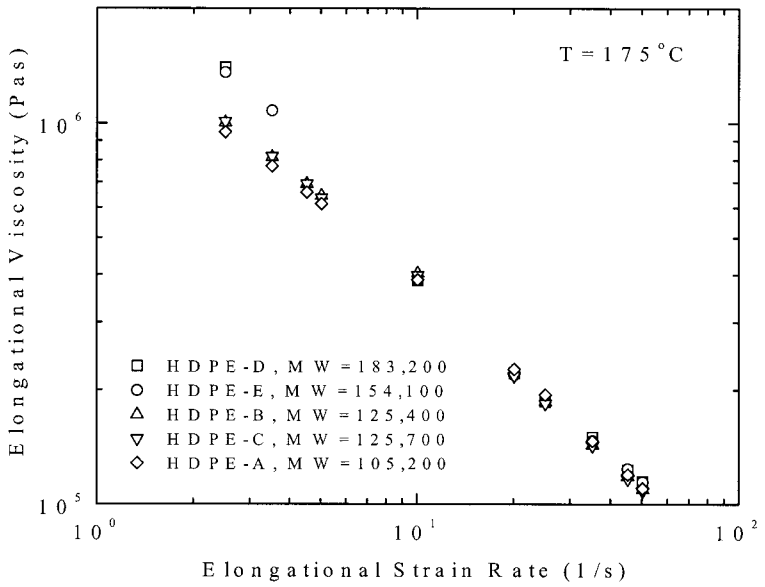

Figure 1 HDPE effective elongational viscosity at 175°C.

ing strain rate. Among the HDPE samples, noticeable differences in the elongational viscosities were observed between groups comprising grades A, B, and C with lower molecular weights and D and E with higher molecular weights. At the lowest elongational strain rate of 2.52 s^{-1}, the relative difference between these two groups was approximately four-tenths of a decade, that is, 400,000 Pa s, and this difference stayed relatively constant with the temperature. However, with increasing strain rate, the viscosity differences appeared to diminish and the lines converged at higher strain rates. The point of convergence was dependent upon temperature in that a low temperature caused an earlier convergence than did a high temperature. For example, at 175°C (Fig. 1), lines converged at about 10 s^{-1}; at 200°C (Fig. 2), at about 20 s^{-1}; and at 225°C (Fig. 3) and at 250°C (Fig. 4), the point of convergence was outside the measured range. For the five HDPE sam-

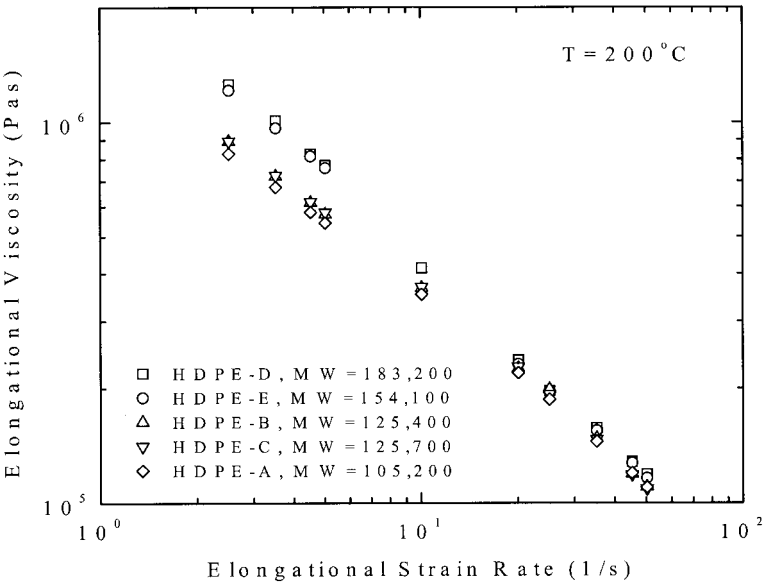

Figure 2 HDPE effective elongational viscosity at 200°C.

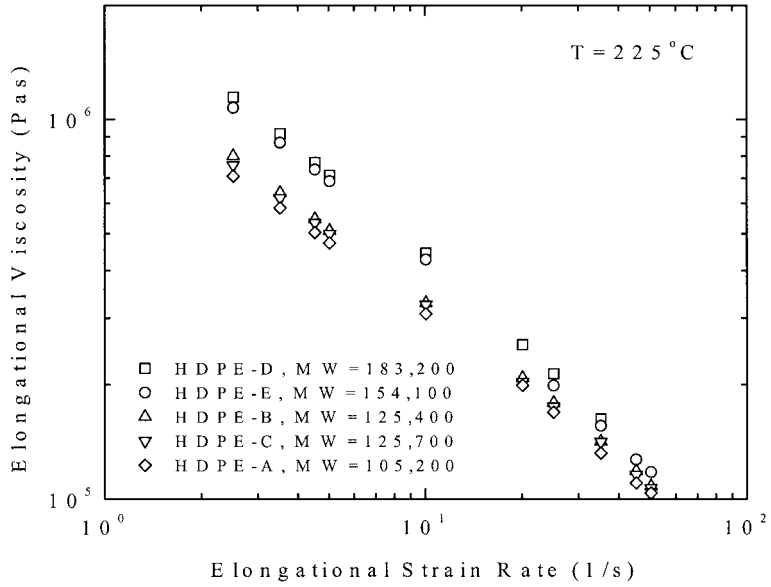

Figure 3 HDPE effective elongational viscosity at 225°C.

ples, the order of magnitude of the viscosity at an equal strain rate followed the order of the magnitude of the molecular weight, that is, grade A with the lowest molecular weight = 105,000 exhibited the lowest viscosity values at rates prior to convergence of the lines. Grades B and C have essentially equal molecular weights with 125,400 and 125,700, respectively, although their densities differ. Indeed, their lines are essentially superimposed. Grades E and D follow in order with molecular weights of 154,100 and 183,200, respectively, having also the highest viscosities. The basically equal molecular weight grades B and C, having different densities, did not exhibit significant viscosity differences. These observations suggest that the molecular weight of HDPE rather than the degree of branching (density) predominantly control the viscosity differences. In fact, HDPEs are linear polyolefins with minor branching characteristics. The long, linear, high

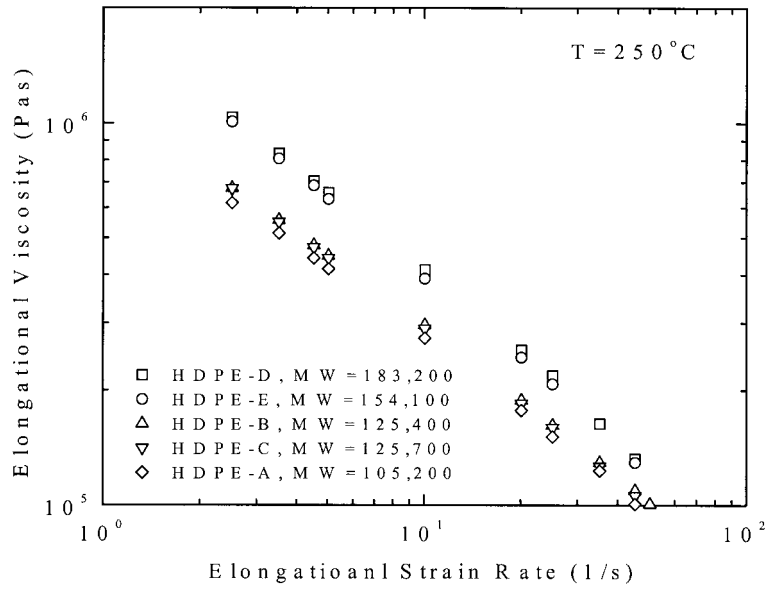

Figure 4 HDPE effective elongational viscosity at 250°C.

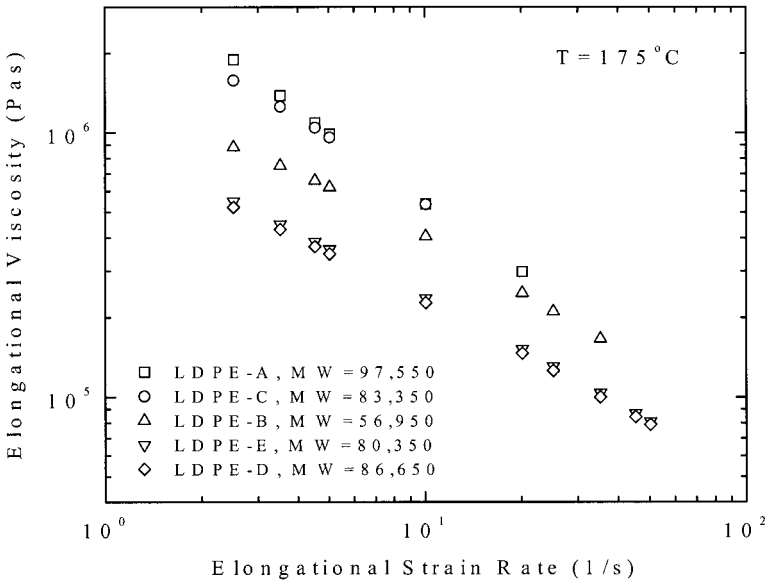

Figure 5 LDPE effective elongational viscosity at 175°C.

molecular weight chains are prone to entangle and, hence, are expected to cause high melt viscosities. The diminishing effect of the molecular influence on the elongational viscosity with an increasing strain rate is thought to be the result of an asymptotic approach to a limiting orientation. The polymer chains are increasingly oriented with respect to each other and are not as influenced by entanglement and sliding effects related to molecular structure as they are at lower strain rates.

LDPE elongational melt viscosities were evaluated under the same aspects (Figs. 5–8). As for the HDPE samples, the melt viscosities were decreasing power-law functions of the strain rate. The previously mentioned converging effect of the viscosity lines can also be seen here, in particular, for the copolymer grades A, B, and C. Again, the molecular weight controlled the spread along the viscosity axis when comparing grade B with a molecular weight = 56,950 versus grades A and C with molecular weights of 97,550 and 83,350, re-

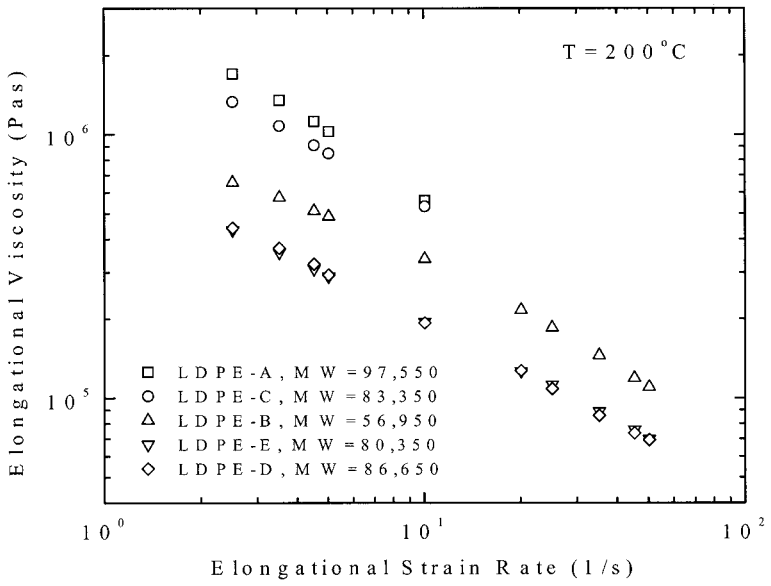

Figure 6 LDPE effective elongational viscosity at 200°C.

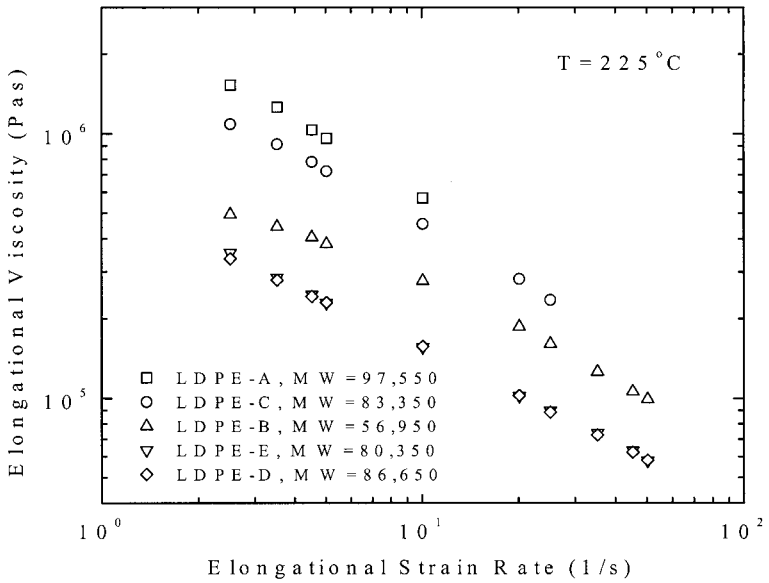

Figure 7 LDPE effective elongational viscosity at 225°C.

spectively. The homopolymer grades D and E at about equal molecular weights of 86,650 and 80,350, respectively, but different densities of 0.919 and 0.923, respectively, were insensitive to strain-rate or temperature variations. This behavior of molecular weight control as opposed to the insignificant branching effect on elongational viscosities as seen for the HDPE samples is again reflected in the comparison of the LDPE samples. It should be noted that the polydispersity of LDPE samples near 2.0 indicates that these samples were metallocene-catalyzed, whereas samples D and E were Ziegler–Natta-catalyzed. The metallocene-catalyzed samples had higher effective elongational viscosities than those of the Ziegler–Natta-catalyzed samples with nearly the same average molecular weights.

It shall be mentioned at this point that the observed differences between elongational viscosities of different grades are greater than are the

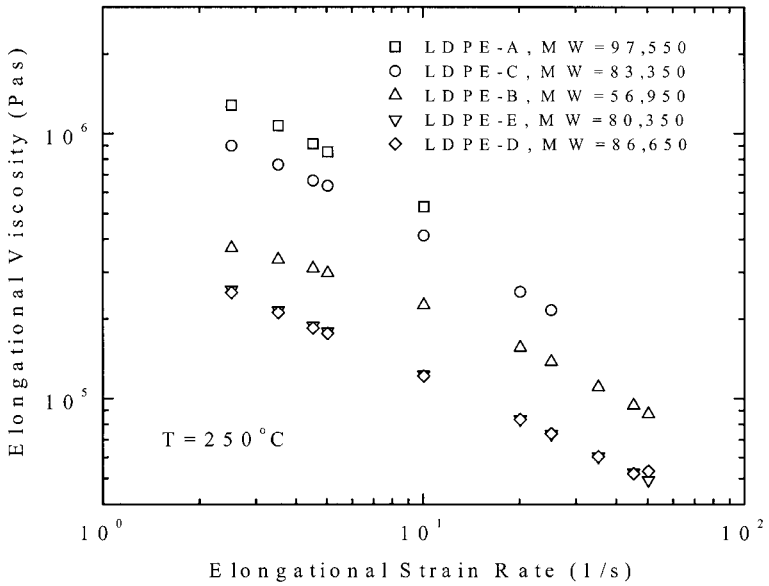

Figure 8 LDPE effective elongational viscosity at 250°C.

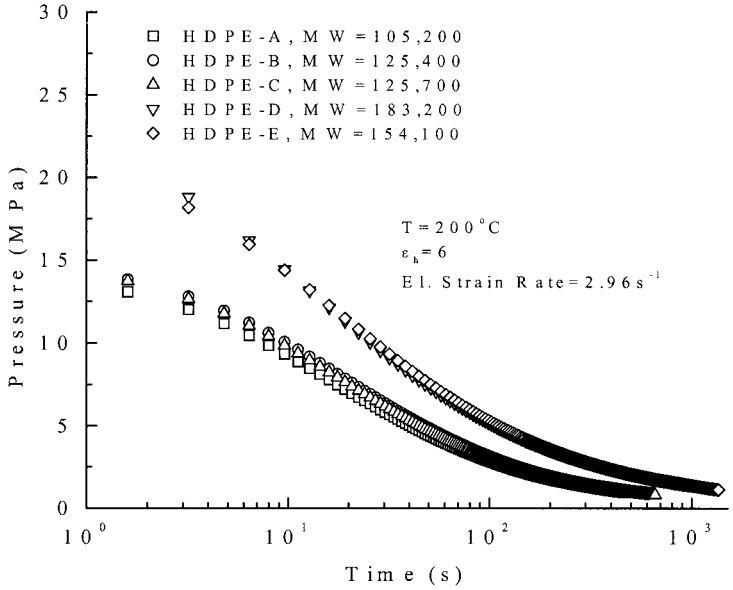

Figure 9 HDPE melt-pressure relaxation at $T = 200°C$, $\varepsilon_h = 6$, $\dot{\varepsilon} = 2.96\ s^{-1}$.

margins of experimental error. Tests have shown that the ACER is an extremely precise instrument that allows for repeated measurements at equal conditions with marginal deviations of usually no more than 1.5%. Therefore, viscosity differences displayed on the logarithmic-scaled figures are the result of variations in the molecular uniqueness rather than seemingly due to potential experimental inconsistencies or errors.

To substantiate the observation of an asymptotic approach to a limiting orientation along with the apparent effects of molecular parameters at a low process strain rate, melt-pressure relaxation was measured at varying elongational strain rates using the ACER. The curves were obtained for the melts extruded through the Hencky 6 semihyperbolic die at 200°C. Graphs were prepared as time-dependent, exponentially decaying pressure functions and were parameter-fitted using Origin® software. Graphs are displayed for the HDPE samples at process strain rates of 2.96, 20.12, and 35.21 s^{-1} in Figures 9–11, respectively. A logarithmic scale was chosen for the time dimension for display purposes, allowing for more spread between the curves and ease of comparison. Figure 9 shows the relaxation spectrum at a low process rate of 2.96 s^{-1}. The curves are second-order decay of the form $P = P_0 + A_1 \exp(-t/\lambda_1) + A_2 \exp(-t/\lambda_2)$, where A_1 and A_2 are the first and second preexponential factors and λ_1 and λ_2 are the first and second time constants, respectively. The first time constant is the location at which the tangent to the onset of relaxation intercepts with the time axis. Estimates show that at this time the pressure has decayed to about 63% of its original value, which is equivalent to $1 - (1/e)$. By nature of the exponential decay function, the rate of decrease is most rapid during the initial short time period. Hence, the first decay constant is an important measure for the extent and rate of relaxation and a useful tool to differentiate between melts of unique molecular characteristics. Table II summarizes the dependence of the first decay constant on the elongational strain rate for pressure relaxation at 200°C and Hencky 6 die geometry. The rate of relaxation should be related to the degree of orientation that has developed prior to relaxation. A large thermodynamic driving force for relaxation will cause the time constants to be smaller for more highly oriented melts as reflected by the time constants at higher strain rates. Moreover, the difference of time constants between strain rates decreases as the elongational strain rate and, hence, the orientation level increases, indicating an asymptotic approach to a limiting value. Evidently, as will be discussed later, the calculated entropy changes for Hencky 6 and 7 extruded samples increased in magnitude with an increasing elongational strain rate, which is indicative of the just-mentioned increase in orientation at asymptotically decreasing relaxation time constants.

Turning to the relaxation curves, for the low strain rate of 2.96 s^{-1} (Fig. 9), the staggered order

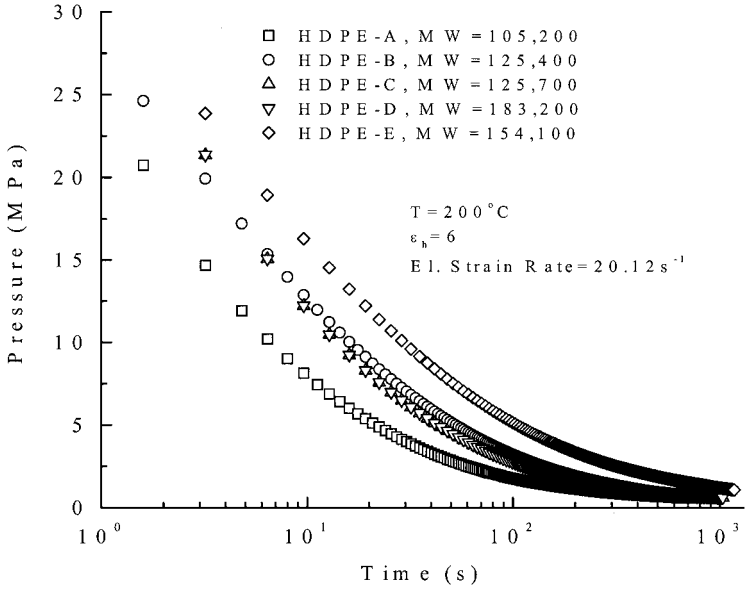

Figure 10 HDPE melt-pressure relaxation at $T = 200°C$, $\varepsilon_h = 6$, $\dot{\varepsilon} = 20.12\ s^{-1}$.

of curves follows the order of the molecular weight in the same way as it did for the elongational viscosities in Figure 2. The two molecular weight groups of HDPE samples A–C and samples D and E are also clearly distinguishable here. As the process strain rate increases to 20.12 s^{-1} (Fig. 10), which is the point of convergence of the elongational viscosities at 200°C as shown in Figure 2, the decay curves become third order. The order of the molecular weight is now more or less random and the two molecular weight groups are not distinguishable anymore, probably due to the effect of the orientation approaching an asymptotic limit, causing the relaxation to be less sensitive to molecular weight effects. At an even higher process rate of 35.21 s^{-1} (Fig. 11), the relaxation curves remain third order and appear yet less ordered. The decreased dependence upon the molecular weight with increasing strain rate reflected in the relaxation spectrum thus conforms

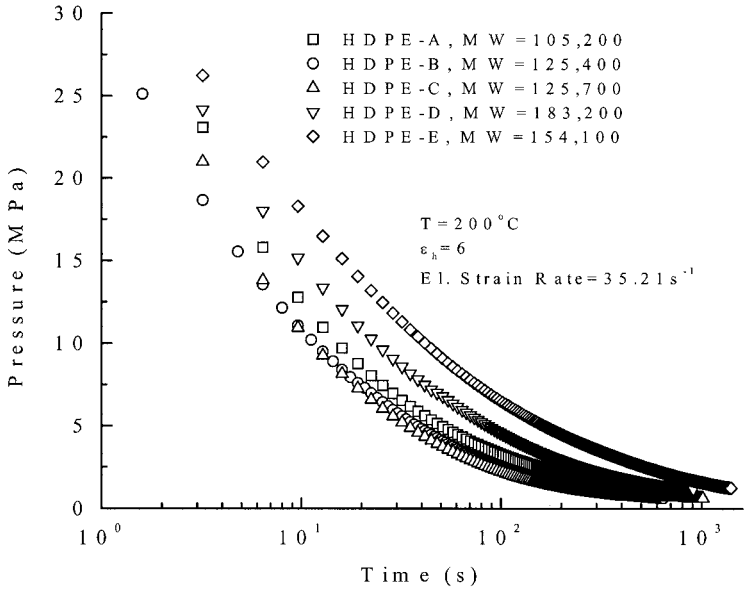

Figure 11 HDPE melt-pressure relaxation at $T = 200°C$, $\varepsilon_h = 6$, $\dot{\varepsilon} = 35.21\ s^{-1}$.

Table II First Decay Constant for HDPEs at 200°C and Hencky 6 Die Geometry

Sample	$\dot{\varepsilon} = 1.04\ s^{-1}$	$\dot{\varepsilon} = 2.07\ s^{-1}$	$\dot{\varepsilon} = 2.96\ s^{-1}$	$\dot{\varepsilon} = 20.12\ s^{-1}$	$\dot{\varepsilon} = 35.21\ s^{-1}$
HDPE-A	26.68	19.09	14.89	4.03	6.01
HDPE-B	32.58	25.42	17.47	5.92	4.06
HDPE-C	28.92	20.89	16.96	7.16	5.73
HDPE-D	37.98	25.46	19.80	7.15	6.16
HDPE-E	43.25	39.72	23.91	8.92	8.44

to the convergence of the strain rate-dependent elongational viscosity lines at higher process strain rates. Hence, at high loads, molecular uniqueness becomes less influential, yielding to orientation development and the associated restructuring of the melt's molecular morphology. Molecular chains start to disentangle and align in a more organized, layered fashion, thereby lowering the melt viscosity.

When comparing the relaxation time constants of Hencky 6 to Hencky 7 extruded melts, no differences were observed other than that the latter were larger in magnitude than were the former, which agrees with the generally higher melt viscosities produced by the Hencky 7 over the Hencky 6 semihyperbolic die. Enthalpy and entropy changes were calculated based on eqs. (14) and (15). To accomplish this task, shear rheological data had to be obtained using the Bohlin shear rheometer in a continuous rotational and oscillatory mode. The shearing range covered shear rates in the order of magnitude equivalent to the elongational strain rates used to obtain data from the ACER. In the case of the HDPE samples, the ACER also had to be used with a linear, $L/D = 20$, die to measure shear viscosities at shear rates that were too high to be obtained from the Bohlin rheometer. When using the straight $L/D = 20$ die, a Bagley entrance correction was performed to correct for the equilibrium pressure offset caused by die entrance effects.

In Figures 12 and 13 are shown the enthalpy and entropy changes, respectively, for HDPE samples. At 200°C, the measured enthalpy and entropy changes increased in magnitude (became more negative) as the process strain rate increased for both die geometries. This may be restated by saying that the melt dissipated more thermal energy at decreasing molecular randomness while the process strain rate was increasing, that is, the melt was increasingly transformed to a more ordered state corresponding to a lower

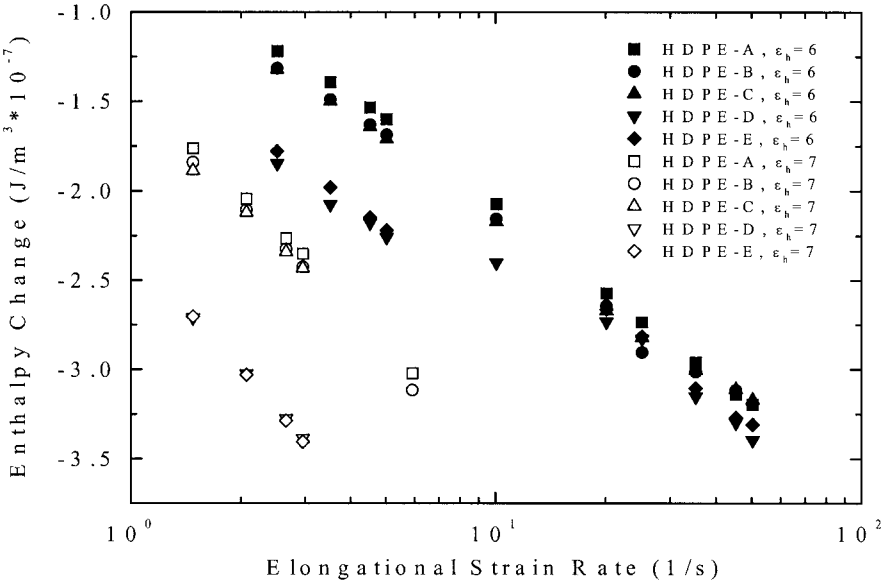

Figure 12 HDPE enthalpy change at 200°C.

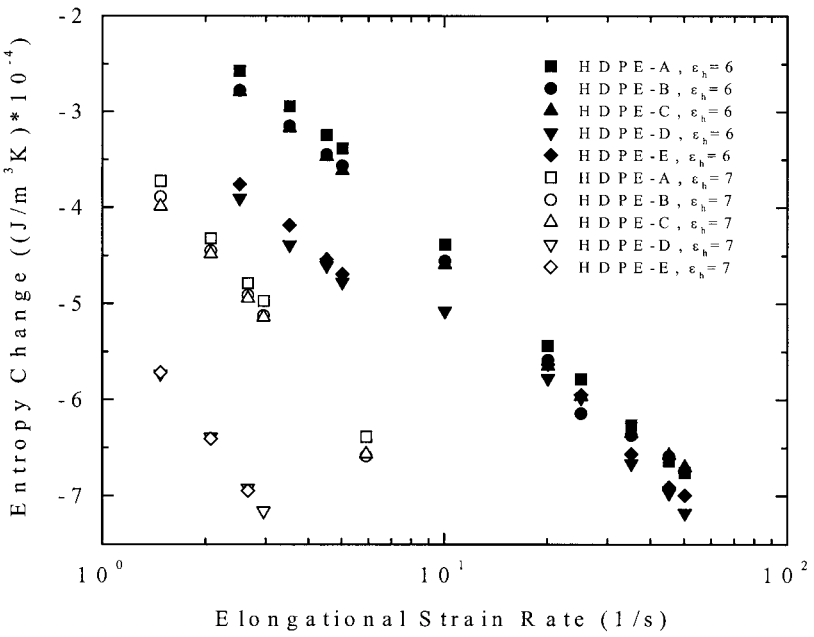

Figure 13 HDPE entropy change at 200°C.

entropy and greater magnitude latent heat of transformation with increasing strain rate. Moreover, at a comparable strain rate, the Hencky 7 extruded melts produced larger enthalpy and entropy changes than did those of the Hencky 6 counterpart. The same was observed for the enthalpy and entropy changes for the LDPE samples at 200°C in Figures 14 and 15. The enthalpy and entropy changes in the HDPE samples indicated a greater magnitude change being required for higher molecular weight samples. The discrimination by molecular weight was more dis-

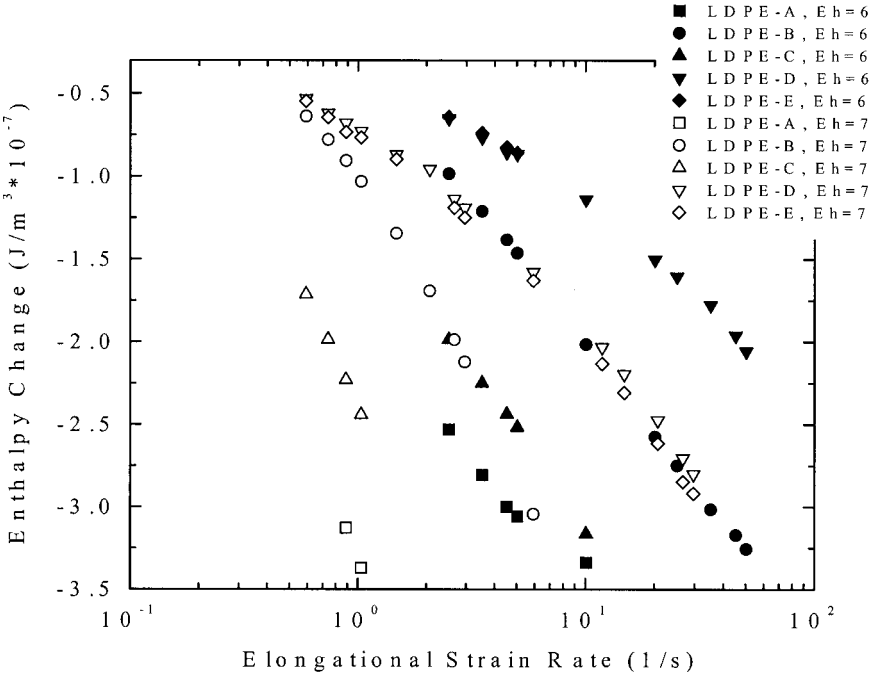

Figure 14 LDPE enthalpy change at 200°C.

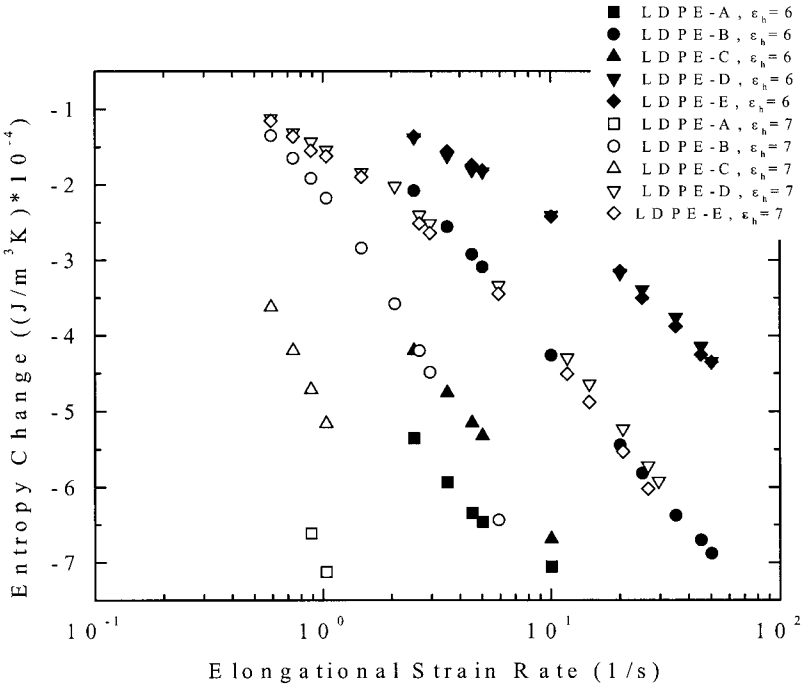

Figure 15 LDPE entropy change at 200°C.

tinct for the Hencky 6 die than it was for the Hencky 7, probably because the increased orientation forced by the more restrictive die dominated the less influential molecular weight contribution. The metallocene-catalyzed LDPE samples having nearly the same relatively high branching content (i.e., density) and polydispersity, samples A, B, and C, indicated the same dependence as that of the HDPE samples on molecular weight and Hencky strain. However, the Ziegler–Natta-catalyzed, less branched, and higher polydispersity LDPE samples, D and E, indicated a significantly smaller magnitude enthalpy and entropy changes than did the other LDPE samples. The HDPE samples, in general, exhibited larger magnitude enthalpy and entropy changes at equivalent lower strain rates than did the LDPE, but all samples seemed to be asymptotically approaching a common limit at higher elongational strain rates. This common limit probably is indicative of a limiting orientation and the rate at which it is approached is dependent upon molecular characteristics.

These general observations suggest that at least flow-induced orientation occurs in a semihyperbolic flow with the extent being dependent upon the elongational strain rate. For Hencky 6 extruded HDPE-A, the enthalpy change ranged from -1.2×10^7 to -3.2×10^7 J/m^3 for a strain rate range from 2.52 to 50.3 s^{-1}. The literature reports[17] for the heat of fusion for PE an experimental value of 8.22 kJ/mol/monomer unit. For the HDPE sample A, this would be equivalent to -2.77×10^8 J/m^3. This last value is one order of magnitude higher as expected for the solid crystalline state having a significantly higher degree of orientation than a possible *meta*-stable liquid form. Collier[14] reported values very much comparable in magnitude with those presented here when investigating flow-induced orientation in polypropylene melts.

CONCLUSIONS

When comparing strain rate-dependent elongational viscosities of the molecularly uniquely characterized HDPE and LDPE samples, it was observed that the elongational viscosity differences were primarily controlled by the molecular weight rather than by the degree of branching and that this effect was process-strain-rate- as well as temperature-dependent. At low elongational strain rates, the viscosity differences among HDPE and LDPE samples were visibly dependent upon the molecular weights, whereas at higher and the highest strain rates, the viscosity differences diminished. To further investigate

the causes of these said observations, pressure melt relaxation curves were recorded, regressed, and parameter-fitted to determine the pressure relaxation time constants. Time constants were observed to decrease with increasing elongational strain rate as well as their relative difference also decreased, indicating that with increasing strain rate the molecular field of the melt asymptotically gained orientation in approaching a limit. As a result of this behavior, molecular uniqueness became much less distinct at high process strain rates, yielding to orientation development and the associated restructuring of the melt's molecular morphology.

In an effort to investigate flow-induced orientation of the PES in semihyperbolic dies, enthalpy and entropy changes were calculated from ACER elongational and continuous rotational as well as oscillatory shear data. With increasing strain rate, the melts released more energy and the molecular structure became more ordered as the enthalpy and entropy changes increased in magnitude. With the Hencky 7 die, larger enthalpy and entropy changes were achieved at equal strain rates than with the Hencky 6 die. Therefore, flow-induced orientation was achieved to an extent dependent upon the Hencky strain and elongational strain rate. The said flow-induced orientation was characterized by an enthalpy change one order of magnitude lower than the heat of fusion.

NOMENCLATURE

b_r body force in r-direction
b_z body force in z-direction
ΔG Gibbs free-energy change
H enthalpy
$\hat{H}$ enthalpy per unit mass
L centerline length of die
P melt pressure
ΔP pressure drop, defined as entrance minus exit pressure
q heat flux
r die radial dimension
r_e radius of die exit
r_o radius of die entrance
ΔS entropy change
t time variable
T temperature
v_0 initial melt velocity
v_r velocity component in r-direction
v_z velocity component in z-direction
z die axial dimension

Greek Symbols

Δ deformation rate tensor
$\dot{\varepsilon}$ elongational strain rate
ε_h Hencky strain as defined in eq. (7)
Φ potential function as defined in eq. (2)
η_e elongational viscosity
η_{ef} effective elongational viscosity as defined in eq. (11)
η_s shear viscosity
ρ melt density
τ stress tensor
τ_{rr} stress tensor in r-direction
τ_{zz} stress tensor in z-direction
Ψ stream function as defined in eq. (1)

REFERENCES

1. Bailey, L. E.; Cook, D. G.; Pronovost, J.; Rudin, A. Polym Eng Sci 1994, 34, 1485.
2. Müller, A. J.; Balsamo, V.; Da Silva, F.; Rosales, C. M.; Saez, A. E. Polym Eng Sci 1994, 34, 1455.
3. Hingmann, R.; Marczinke B. L. J Rheol 1994, 38, 573.
4. Wagner, M. H.; Bernnat A. J Rheol 1998, 42, 917.
5. Okamoto, M.; Kubo, H.; Kotaka, T. Polymer 1998, 39, 3135.
6. Okamoto, M.; Kubo, H.; Kotaka, T. Macromolecules 1998, 31, 4223.
7. Patel, R. M.; Bogue, D. C. J Rheol 1989, 33, 607.
8. Ramanan, V. V.; Bechtel, S. E.; Gauri, V.; Koelling, K. W.; Forest, M. G. J Rheol 1997, 41, 283.
9. Levitt, L.; Macosko C. W. J Rheol 1997, 41, 671.
10. Takashai, T.; Takimoto, J.; Koyama K. J Appl Polym Sci 1998, 69, 1765.
11. Greener, J.; Evans, J. R. G. J Rheol 1998, 42, 697.
12. Neumann, R. M. J Chem Phys 1999, 110, 7513.
13. Burghard, W. R.; Li, J.; Khomami, B.; Yang, B. J Rheol 1999, 43, 147.
14. Collier, J. R.; Romanoschi, O.; Petrovan, S. J Appl Polym Sci 1998, 69, 2357.
15. Kim, H. C.; Pendse, A.; Collier, J. R. J Rheol 1994, 38, 831.
16. Bird, R. B.; Stewart, W. E.; Lightfoot, E. N. Transport Phenomena; Wiley: New York, 1960.
17. Van Krevelen, D. W. Properties of Polymers; Elsevier: New York, 1990.